IOPscience iopscience.iop.org

Home Search Collections Journals About Contact us My IOPscience

Spindle checkpoint regulated by nonequilibrium collective spindle-chromosome interaction; relationship to single DNA molecule force-extension formula

This article has been downloaded from IOPscience. Please scroll down to see the full text article.

2009 J. Phys.: Condens. Matter 21 502101

(http://iopscience.iop.org/0953-8984/21/50/502101)

View the table of contents for this issue, or go to the journal homepage for more

Download details:
IP Address: 129.252.86.83
The article was downloaded on 30/05/2010 at 06:24

Please note that terms and conditions apply.

IOP FTC
IOP Publishing
Journal of Physics: Condensed Matter
J. Phys.: Condens. Matter **21** (2009) 502101 (9pp)
doi:10.1088/0953-8984/21/50/502101

FAST TRACK COMMUNICATION

Spindle checkpoint regulated by non-equilibrium collective spindle-chromosome interaction; relationship to single DNA molecule force-extension formula

Leif Matsson

Department of Physics, University of Gothenburg, SE-412 96 Göteborg, Sweden

E-mail: leif.matsson@telia.com

Received 1 July 2009, in final form 17 September 2009
Published 13 November 2009
Online at stacks.iop.org/JPhysCM/21/502101

Abstract
The spindle checkpoint, which blocks segregation until all sister chromatid pairs have been stably connected to the two spindle poles, is perhaps the biggest mystery of the cell cycle. The main reason seems to be that the spatial correlations imposed by microtubules between stably attached kinetochores and the nonlinear dependence of the system on the increasing number of such kinetochores have been disregarded in earlier spindle checkpoint studies. From these missing parts a non-equilibrium collective spindle–chromosome interaction is obtained here for budding yeast (*Saccharomyces cerevisiae*) cells. The interaction, which is based on a non-equilibrium statistical mechanics, can sense and count the number of stably attached kinetochores and sense the threshold for segregation. It blocks segregation until all sister chromatids pairs have been bi-oriented and regulates tension such that segregation becomes synchronized, thus explaining how the cell might decide to segregate replicated chromosomes. The model also predicts kinetochore oscillations at a frequency which agrees well with observation. Finally, a relationship between this spindle–chromosome dynamics and the force-extension formula obtained in a single DNA molecule experiment is obtained.

S Supplementary data are available from stacks.iop.org/JPhysCM/21/502101/mmedia

1. Introduction

An understanding of the mechanism by which cells decide to block or permit segregation of replicated chromosomes would not only improve the knowledge about normal cells but almost certainly also give better insight into cancerous cell division. This mechanism, the so-called spindle checkpoint, blocks segregation until all sister chromatid (SC) pairs have been (bi-oriented) stably attached at their kinetochores by microtubules (MTs) from the two spindle poles and assembled (aligned) at the metaphase plate [1–6] (figure 1). Kinetochores are highly specialized protein complexes assembled on centromeric DNA [7–9]. It is thought that the spindle checkpoint could monitor the kinetochore–spindle interaction [4], which, apart from MTs and kinetochores, is mediated by different molecular motors and many other proteins [1, 5, 8]. However, three conditions that uniquely determine the form of this interaction have been disregarded in earlier spindle checkpoint studies: (1) the spatial correlations induced by the MTs and the two spindle poles between the stably attached kinetochores and between the forces acting on them, (2) the non-equilibrium equation for attachment of MT plus-ends to kinetochores and (3) the initial boundary constraints for these two reactants. Without spatial correlations that generate position-dependent forces, bi-oriented SC pairs could not assemble on the metaphase plate [5, 8] and without the increase in attachments the cell could not reach the segregation threshold. In the absence of spatial correlations and initial constraints the cell could not sense and count the number of stably attached kinetochores and could not sense the

 © 2009 IOP Publishing Ltd Printed in the UK

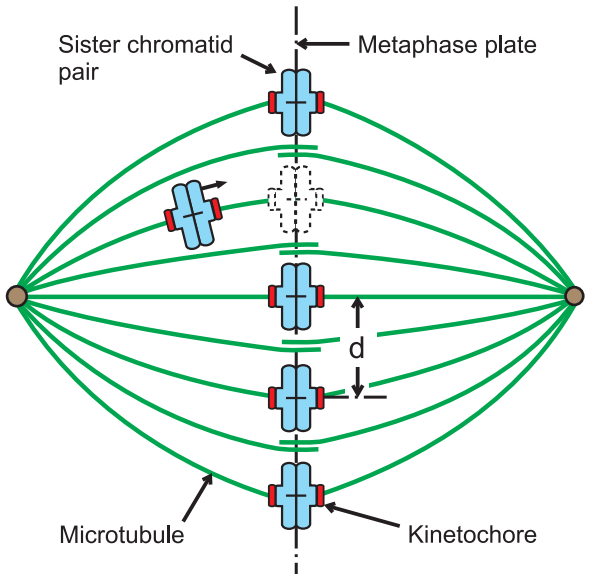

Figure 1. Schematically depicted mitotic spindle in late metaphase. The two spindle poles are located on the x_1-axis and the metaphase plate in the x_2x_3 plane. In budding yeast the kinetochores are more clustered around the centre of mass, $\boldsymbol{r}_{\rm cm} = (0, 0, 0)$, rather than dispersed on the metaphase plate, hence $d \approx 0$. The kinetochore cluster is then stretched along the $x_1 \equiv x$ axis and the spacing in this one-dimensional 'lattice' is $\Delta_1 \equiv \Delta$. Once the last SC pair is bi-oriented and located at the metaphase plate, APC is activated by Cdc20 and the SC pairs synchronously separated.

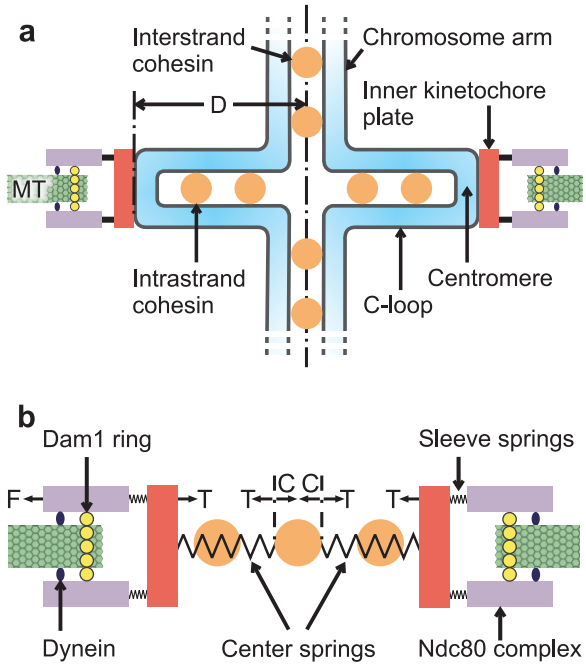

Figure 2. Bi-oriented sister chromatid pair. (a) Chromosome arms are tethered by interstrand cohesin and C-loops by intrastrand cohesion. (b) Centromeric tension T is balanced by cohesive forces C from interstrand cohesin, which connects the two centre springs representing the C-loops, and by poleward forces F generated and regulated by the stably connected part of the spindle–SC system. The stably attached MT is enclosed by a sleeve-like complex of Ndc80 and Dam1 ring proteins, and connected to the inner kinetochore plate by sleeve springs.

segregation threshold. The spindle checkpoint problem has been obscured also by variable chemical and dynamic properties of MTs and kinetochores [7–9], such as the rapid growth and shrinkage ('dynamic instability') of MTs [10] and the poleward movement of tubulin [11].

When an SC pair is bi-oriented the attaching MTs exert opposite pulling forces on the two sister kinetochores, generating tension in the centromeric chromatin loops (C-loops) [12] (figure 2). Only kinetochore-MT arrangements that create normal tension become stabilized [6, 13]. Centromeric tension is in turn balanced by cohesive forces (figure 2), which are mediated by cohesin protein complexes that keep the SCs tethered in pairs [14–16] before and during the spindle–SC assembly [17, 18]. The removal of cohesin is induced by the anaphase-promoting complex (APC), after activation by a protein Cdc20 and phosphorylation by kinases such as Cdk1 and Plk1 [1]. In the absence of tension, after phosphorylation of some kinetochore protein subunits by kinases, such as Mps1, Ilp1/Aurora B and Plk1, unattached kinetochores bind Cdc20 with Mad and Bub proteins in a mitotic checkpoint complex (MCC) [1, 2, 8], explaining how the blocking mechanism works at a single kinetochore. But how this machinery works collectively and quantitatively has been classed as one of the big mysteries of the cell cycle [2]. The combination of the non-equilibrium attachment reaction and the initial boundary constraints with the spatial correlations, which induces a nonlinear cooperative type dynamics driven by the increasing number of stably attached kinetochores, places the spindle checkpoint problem in an unexplored gap between molecular biology and condensed matter physics [19].

A solution, a non-equilibrium collective spindle–SC interaction, is obtained here for budding yeast (*S. cerevisiae*). In this case a single MT attaches to each kinetochore [4], making the problem simpler compared to other species. The collective interaction, which is based on a non-equilibrium statistical mechanics, can sense and count the number of stably attached kinetochores. It senses the threshold for segregation, blocks segregation until all SC pairs have been bi-oriented and regulates tension and cohesion such that segregation is synchronized [1]. The model thus provides answers as to how the spindle checkpoint machinery could work and how the cell might decide to segregate replicated chromosomes. It also predicts kinetochore oscillations at a frequency that agrees well with observation [20]. Finally, a relationship between the obtained collective spindle–DNA dynamics and the force-extension formula [21] assessed on a single DNA molecule in the laboratory is obtained.

2. A non-equilibrium statistical mechanics

The dynamic instability of MTs ensures a rapid regulation of the key reactant densities, a prerequisite for a successful spindle assembly [5]. But it has not been possible to link any of the variable chemical and dynamic properties of the spindle–SC system [5, 7–11] to the quantitative behaviour of the spindle checkpoint machinery, i.e. to the switch-like all-or-none transition to anaphase once all SC pairs have been

bi-oriented [4]. Therefore, instead of an attempt to model the regulation of the key reactants in detail, it might be a better strategy to formulate a dynamics in terms of their bulk properties.

It seems reasonable to assume that the volume average density ψ of kinetochores attached by MT plus-ends during the spindle assembly should increase linearly with each of the volume average densities of MT plus-ends ρ and vacant kinetochores σ according to

$$\frac{\mathrm{d}\psi}{\mathrm{d}t} = k\rho\sigma - k'\psi, \tag{1}$$

k and k' being the on and off rate constants. The two reactant densities depend on each other via the initial boundary conditions, $\rho_0 = \rho + \psi$ and $\sigma_0 = \sigma + \psi$, where ρ_0 and σ_0 are the initial reactant densities. With these constraints inserted equation (1) becomes

$$\frac{\mathrm{d}\psi}{\mathrm{d}t} = k((a-\psi)^2 - (a^2 - b^2)), \tag{2}$$

where $a = (\rho_0 + \sigma_0 + K)/2$, $K = k'/k$ and $b^2 = \rho_0\sigma_0$. As ρ denotes only the MT plus-ends, equations (1) and (2) should hold, regardless of from which MT organizing centre the MTs grow and when these centres reduce to the two spindle poles (figure 1) [17, 22]. By removing inappropriate attachments, apart from an impact on turnover of reactant densities, Ilp1/Aurora B can increase k' [4, 7] and promoters of MT nucleation and stabilization, such as GTPase Ran [17] and CLASP proteins [7], can increase k. By transporting mono-oriented SC pairs to the metaphase plate, CENP-E motor proteins too can increase k [18]. The solution to equation (2) is

$$\ln\left(\frac{\rho'}{\sigma'}\frac{\sigma_K}{\rho_K}\right) = k(\rho_K - \sigma_K)t \equiv 2kagt, \tag{3}$$

where $\rho' = \rho_K - \psi$ and $\sigma' = \sigma_K - \psi$ are here called 'dynamic' reactant densities, $\rho_K = a(1+g) > \rho_0$ and $\sigma_K = a(1-g) < \sigma_0$ 'screening' and 'screened' reactant densities (figure 3), and $g^2 = (a^2 - b^2)/a^2$. Hence $\rho_K = \rho' + \psi$ and $\sigma_K = \sigma' + \psi$ work as dynamic boundary constraints.

In the high affinity limit ($k' \to 0$), where ρ_K, σ_K, ρ' and σ' become the usual reactant densities, ρ_0, σ_0, ρ and σ, equation (3) and the following calculations would become much simpler. But as detachment is crucial for the polar ejection forces and the spindle assembly [5], k' is kept nonzero. The density of MT plus-ends is much larger than that of kinetochores, $\rho_K \gg \sigma_K$, hence $g = (\rho_K - \sigma_K)/(\rho_K + \sigma_K) \approx 1$. However, g will play a role as a coupling constant in the spindle–SC interaction and is therefore kept different from one throughout the calculations. Despite the variable chemical and dynamic properties of kinetochores and MTs [5, 7–11] the system becomes sufficiently rigid to create position-dependent forces [5], without which bi-oriented SC pairs would not be able to correlate spatially at the metaphase plate. However, spatial correlations combined with the non-equilibrium chemical reaction (equation (2)) create in turn problems beyond the established knowledge in physics.

Under conditions of chemical equilibrium ($\mathrm{d}\psi/\mathrm{d}t = 0$), $\psi(\boldsymbol{r})$ would be a constant in time, hence normalizable,

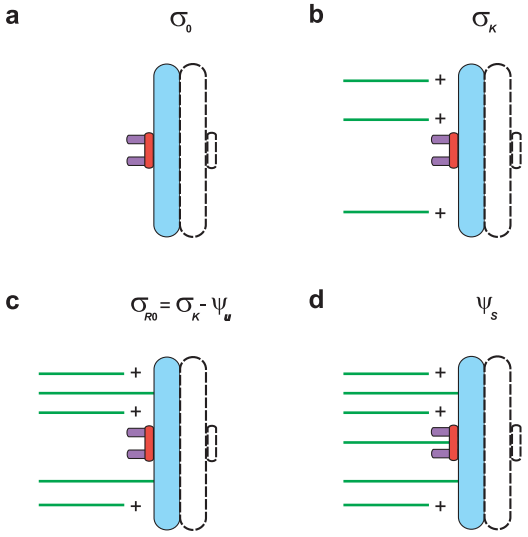

Figure 3. The different kinetochore densities. (a) Bare kinetochore. (b) Kinetochore screened by three unattached MT plus-ends. (c) Previous kinetochore unstably attached by two MTs. (d) Previous kinetochore stably attached by an MT from one of the two spindle poles. The sister chromatids (dotted lines) are exposed to the same mixture of adjacent MT plus-ends.

$\int \psi(\boldsymbol{r})\,\mathrm{d}\boldsymbol{r} = 1$, and proportional to the probability density of finding one stably attached kinetochore at an arbitrary site $\boldsymbol{r} = (x_1, x_2, x_3)$. The conformational distribution of a 'lattice' of n such complexes at sites $\boldsymbol{r}_\lambda$ could then be written as in the freely jointed chain (FJC) model [23], $\varphi = \mu\psi(\boldsymbol{r}_1)\psi(\boldsymbol{r}_2)\psi(\boldsymbol{r}_3)\cdots\psi(\boldsymbol{r}_n)/a^n$. In the actual system the unstable attachment density ψ_u becomes a constant in time, hence normalizable, when the rate of detachment equals that of the unstable attachment, $\mathrm{d}\psi_\mathrm{u}/\mathrm{d}t = 0$. However, the density of stably attached kinetochores ψ_s increases with time and is therefore not normalizable, hence proportional to the probability density of finding between zero and any integer or fractional number of stably attached kinetochores at $\boldsymbol{r}_\lambda$. Therefore, to ensure a given number of stably attached kinetochores, the FJC distribution must be averaged over all orders:

$$\varphi = \mu\sum_{n=0}^{\infty}\left(\frac{1}{a}\right)^n\prod_{\lambda=0}^{n}\psi(r_\lambda, t), \tag{4}$$

where $\psi(\boldsymbol{r}_\lambda, t) = \psi_\mathrm{s}(\boldsymbol{r}_\lambda, t) + \psi_\mathrm{u}(\boldsymbol{r}_\lambda)$. The zeroth-order term, $\Delta\varphi = \mu\psi(\boldsymbol{r}_0, t) = \mu$, accounts for unstable attachments before stable attachment has started. The network of almost rigid stably attached MTs should inhibit rapid oscillatory movements of individual stably attached kinetochores. As the average transport of SC pairs is directed towards the metaphase plate [5, 17, 18] pair-wise oscillations of sister kinetochores should also be absent in the average forces. Accordingly, the system should be dominated by a 'slower' dynamics in which the average spacing between stably attached kinetochores, $\langle|\Delta x_{i\lambda}|\rangle = \Delta_i$, the lattice lengths L_i and all distances shorter than a certain 'coherence length' l, can be neglected in comparison with an infinitely long 'wavelength' of 'zero-frequency' oscillations (absence of oscillations). As ψ is then

space-independent equation (4) becomes

$$\varphi = \mu \sum_{n=0}^{\infty} \left(\frac{\psi}{a}\right)^n = \frac{\mu}{1-\psi/a}, \tag{5}$$

as if all kinetochores were clustered in one point. The time derivative of φ becomes

$$\frac{\mathrm{d}\varphi}{\mathrm{d}t} = \frac{\mu}{a}\frac{1}{(1-\psi/a)^2}\frac{\mathrm{d}\psi}{\mathrm{d}t}, \tag{6}$$

which shows that the non-equilibrium attachment reaction (equation (2)) controls the entire system in the limit of slowly varying dynamics. Interestingly, equation (5) corresponds formally to the grand partition function in equilibrium statistical mechanics and ψ/a to the fugacity [24], which is here regulated by the non-equilibrium attachment reaction (equation (2)).

But the question is if kinetochores actually become clustered in space. Yes, clusters of kinetochores are observed in budding yeast [8]. A contact within the distance l between an MT plus-end and a kinetochore, whether mediated by a protein, a chromosome arm or an MT (figure 4), should hence be counted as point-like in the sense of equation (1), the crucial question being if physical contact has been established or not. Such contacts, involving chromokinesins [25, 26] and chromosome arms, induce the polar ejection forces (figure 4), which transport SC pairs to the metaphase plate [5, 26]. Cytoplasmic dynein motor proteins [27] and MT depolymerization in kinetochores [28] are thought to move the SC pairs polewards until the increasing density of MTs near the spindle poles makes the polar ejection forces strong enough to move the SC pairs back antipolewards (figure 1), creating an oscillatory movement [25, 29–31]. But as mentioned before, the average transport of SC pairs is directed towards the metaphase plate [5, 17, 18], suggesting that the collective spindle–SC interaction is independent of such 'directional instability' effects [30]. In this average dynamics the transport of bi-oriented SC pairs to the metaphase plate is reduced to a time lag.

3. A collective spindle–chromosome interaction

By insertion of equation (2), equation (6) yields the time evolution of the total number $\varphi = \varphi_s + \varphi_u$ of stable and unstable attachments in the spindle volume:

$$\frac{\mathrm{d}\varphi}{\mathrm{d}t} = \frac{ka}{\mu}(\mu^2 - g^2\varphi^2), \tag{7}$$

which has the solutions $\varphi(t) = \pm(\mu/g)\tanh(kagt)$ and $\varphi = \pm\mu/g$. To ensure that all SC pairs have been bi-oriented and assembled at the metaphase plate, they must be exposed to MT plus-ends for a sufficiently long time $2t_0$. This requirement and normalization of φ can be accounted for by a so-called topological quantization [32], $\varphi_s(t_0) - \varphi_s(-t_0) = 2N = 2\mu/g$, $t_0 \gg 1/kag$, whereby $\Delta\varphi$ is automatically subtracted out. N then becomes the total number of bi-oriented SC pairs, ensuring that the correct number of chromosomes will be segregated.

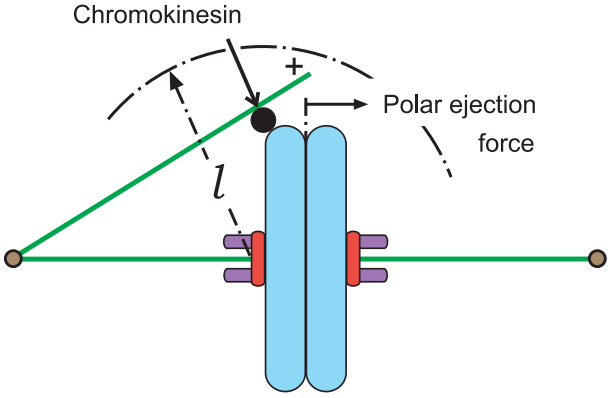

Figure 4. Polar ejection forces. In the spatially coherent approximation all physical contacts within a certain radius l (coherence length) between a kinetochore and an MT plus-end are counted as point-like in the sense of equation (1). Polar ejection forces are transferred via such contacts mediated by MTs, chromosome arms and chromokinesin motor proteins.

A detailed dynamics in three spatial dimensions would probably be more complex than a liquid crystal system [19]. But the genome conserving solution $\varphi(t)$ can also be interpreted as a travelling wave $\xi(x_i) = \varphi/N = \tanh(gx_i/\Delta_i)$ that describes the growth of the 'lattice' of stably attached kinetochores in the continuum limit ($\Delta_i = L_i/2N \to 0$) [33], $x_i = tv_i$ and $v_i = \Delta_i ka$ being the path and velocity of the wave along the x_i axis. Such a form of bi-orientation may appear too ordered in comparison with the real case, however, the travelling wave solution emerges in the spatially coherent dynamics ($\Delta_i \approx 0$) near the spindle checkpoint where the actual order should be less important. In *S. cerevisiae* kinetochores appear to be clustered at the centre of mass $\boldsymbol{r}_{\mathrm{cm}} = (0, 0, 0)$ on the metaphase plate rather than dispersed [8]. Moreover, as the cluster is then extended along the x_1 axis perpendicular to the metaphase plate (figure 1) the spatial index can be dropped. The travelling wave equation is obtained from equation (7), $(1/v)\mathrm{d}\xi/\mathrm{d}t = \mathrm{d}\xi/\mathrm{d}x = g(1-\xi^2)/\Delta \equiv (2V_0)^{1/2}$, but can also be generated by the double-well potential $V_0(\xi) = g^2(1-\xi^2)^2/(2\Delta^2)$ [32] which is symmetric under inversion, $\xi \to -\xi$. It will be interesting to see if this potential can generate also other spindle checkpoint properties and functions.

The derivative of $(\mathrm{d}\xi/\mathrm{d}x)^2 = 2V_0$, $2(d^2\xi/\mathrm{d}x^2)\,\mathrm{d}\xi/\mathrm{d}x = 2(\mathrm{d}V_0/\mathrm{d}\xi)\,\mathrm{d}\xi/\mathrm{d}x$, yields the static part of the second-order equation of motion of the actual lattice in the continuum limit [32, 33]:

$$\eta\frac{\mathrm{d}^2\xi}{\mathrm{d}t^2} - \varepsilon\frac{\mathrm{d}^2\xi}{\mathrm{d}x^2} = -\varepsilon\frac{\mathrm{d}V_0}{\mathrm{d}\xi}, \tag{8}$$

where the time-dependent term corresponds to the acceleration in Newton's force law, $\eta = \varepsilon/s^2$ is the linear mass density, ε the elastic modulus, ξ the deformation (average lattice stretch) and s the velocity for propagation of kinetochore oscillations [20] which in *S. cerevisiae* should be damped out during the metaphase where chromosome arms in SC pairs are still tethered by cohesin [34]. Before anaphase entry, each attachment should then create an equal stretch D in

centromeric chromatin along the x axis (figure 2(a)). The variable ξ can then also denote the average stretch $\chi/D = \langle\chi_\lambda/D\rangle = \Sigma(\chi_\lambda/D)/2N$, where χ_λ is $2D$, D or 0 if the λth kinetochore belongs to a bi-oriented (figure 2(a)), mono-oriented or unattached SC pair, respectively. The non-equilibrium free energy density is defined by the Hamiltonian, $H = \eta(\mathrm{d}\xi/\mathrm{d}t)^2/2 + \varepsilon(\mathrm{d}\xi/\mathrm{d}x)^2/2 + \varepsilon V_0(\xi)$ [35], which shows that the entire system is symmetric under inversion of ξ.

4. Kinetochore oscillations

About 5 min after the start of anaphase the stably attached kinetochores are observed to oscillate at a frequency $f = 1\ \mathrm{min}^{-1}$ [20]. To see if this oscillation can be described by the collective spindle–SC interaction, a time-dependent solution $\xi(x,t) = \xi(x) + \mathrm{e}^{\mathrm{i}\omega t}\zeta(x)$ is inserted in equation (8). Linearization around small perturbations $\zeta(x)$ gives a Schrödinger-like equation $(-d^2/\mathrm{d}x^2 + V_0''(\xi))\zeta_n(x) \equiv (-d^2/\mathrm{d}x^2 + 4g^2/\Delta^2 - 6(g^2/\Delta^2)/\cosh^2(gx/\Delta))\zeta_n(x) = (\omega_n^2/s^2)\zeta_n(x)$ which is exactly solvable [32]. It yields a discrete spectrum, $f_n = \omega_n/2\pi = sg\sqrt{(n(4-n))}/(2\pi\Delta)$, $n = (0, 1)$, and a continuum, $\omega_q^2 = (4+q^2)s^2g^2/\Delta^2$, where $\omega_{\mathrm{th}} = 2sg/\Delta$ is a so-called branch point which here works as a threshold for segregation of the SC pairs and $q \geqslant 0$ determines the velocity of the segregated chromosomes. An estimate of the spacing Δ between kinetochores and of the velocity s for propagation of oscillations in the lattice will show if the frequency derived from the model has the same order of magnitude as the frequency observed.

As tension variations in MTs can propagate almost instantly at over 100 m s^{-1} [36], the time for such perturbations can be neglected. The velocity in chromatin is assumed to be equal to that of anaphase centromere movement in an SC pair, $s \approx (0.33 \pm 0.16)\ \mu\mathrm{m\ min}^{-1}$ [20]. After 5 min in anaphase kinetochores have thus travelled at most $(1.65 \pm 0.8)\ \mu$m from the metaphase plate, implying that the 32 kinetochores are spread out within some $(3.3 \pm 1.6)\ \mu$m about the metaphase plate with an average spacing $\Delta \approx (0.103 \pm 0.050)\ \mu$m. With $g \approx 1$ the discrete spectrum thus predicts stable kinetochore oscillations at $n = 1$, $f \approx \sqrt{3}sg/(2\pi\Delta) \approx (0.88 \pm 0.43)\ \mathrm{min}^{-1}$ (wavelength $\lambda = s/f \approx 0.38\ \mu$m). However, as the model describes an approximate average type dynamics, these numbers should be taken with caution. The zero frequency at $n = 0$ corresponds to the assumption that oscillations do not contribute to the average dynamics. The threshold for segregation, $\omega_{\mathrm{th}} = 2\pi f_{\mathrm{th}} = 2sg/\Delta$, which can also be obtained from the discrete spectrum at $n = 2$ [32], can be viewed as an attempt of the system to oscillate at a 'frequency' $f_{\mathrm{th}} = sg/(\pi\Delta) \approx (1.02 \pm 0.49)\ \mathrm{min}^{-1}$ ('wavelength' $\lambda_{\mathrm{th}} = s/f_{\mathrm{th}} \approx 0.32\ \mu$m), however, at which the SC pairs become separated.

5. A nonlinear elastically braced string of chromatin

The symmetric dynamics yields two 'unphysical' features: (1) the system is excited, $V_0(0) \neq 0$, in the absence of stable attachments (at $\xi = \varphi/N = 0$) and (2) the number of stably attached kinetochores is negative, $\xi = \varphi/N < 0$, for $t < 0$.

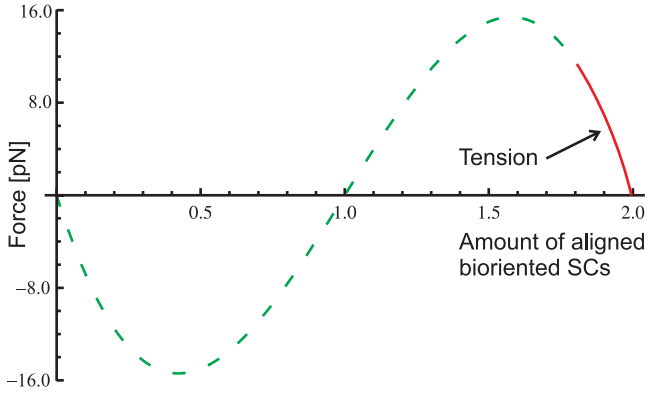

Figure 5. The tension–attachment relationship. Curve denoting the average force F as a function of ξ, the number of stably attached kinetochores relative to the total number N of bi-oriented sister chromatid pairs. In budding yeast ($N = 16$) F becomes a good approximation of the actual tension in the interval $1.8 \leqslant \xi \leqslant 2.0$ where only one SC pair remains to be bi-oriented.

However, these flaws are removed when all SC pairs have been stably attached to the two spindle poles. Mediated by kinetochore oscillations, the spindle–SC system can then relax by a spontaneous shift of order parameter, $\xi \to -1 + \xi$, implied by the instability of the local maximum of $V_0(\xi)$ at $\xi = 0$. After this shift the number of stably attached kinetochores is positive definite, $\varphi(t) \geqslant 0$, at all times and the shifted potential $V(\xi) = D^2\varepsilon g^2\xi^2(2-\xi)^2/(2\Delta^2)$ vanishes in the absence of attachments (at $\xi = 0$).

Equation (8) multiplied by D^2 then becomes

$$D^2\eta\frac{\mathrm{d}^2\xi}{\mathrm{d}t^2} - D^2\varepsilon\frac{\mathrm{d}^2\xi}{\mathrm{d}x^2} = -\frac{\mathrm{d}V}{\mathrm{d}\xi} \equiv F(\xi) = -\frac{\kappa}{2}\xi(1-\xi)(2-\xi), \tag{9}$$

where $\kappa = 4D^2\varepsilon g^2/\Delta^2 = Dk_{\mathrm{sp}}$ is the effective spring constant, $k_{\mathrm{sp}} = 0.1\ \mathrm{pN\,nm}^{-1}$ [31] the Hookean spring constant and $D = 400$ nm [20], hence $\kappa = 40$ pN. Equation (9) thus describes the lattice of stably attached kinetochores along the x-axis as a nonlinear elastically braced string [35] of 'overlapping' centromere flanking chromatin loops, which together with MTs, kinetochore proteins, cohesin and histones [37] determine the elasticity. The average force $F(\xi)$ (figure 5) acting on and between (figure 2) sister kinetochores, and hence also tension, now vanish at $\xi = 0$ and $\xi = 2$ as required by a realistic model.

When no kinetochores ($\varphi = 0$, $\xi = 0$) are stably attached, and when all SC pairs ($\varphi = 2N$, $\xi = 2$) are bi-oriented and assembled at the metaphase plate, F equals the actual but vanishing tension. But already when $N - 1$ SC pairs have been bi-oriented ($\varphi = 2N - 2$), $F(\varphi/N)$ is approximately equal to the actual centromeric tension (figure 5) and hence to cohesion (figure 2(b)), because then only one SC pair remains to come under tension. The collective force $F(\varphi/N)$ then describes how the remaining tension and hence cohesion become equally shared between bi-oriented SC pairs and how tension and cohesion depend nonlinearly on the number of stable attachments [4]. The equal sharing of cohesion ensures

in turn stability in all bi-oriented SC pairs in metaphase [6, 13] and thereby a synchronized vanishing of tension and cohesion by a simultaneous removal of the last linkages at the telomeres. By this genome-wide control of tension and cohesion across sister centromeres, the collective spindle–SC interaction thus blocks segregation until all SC pairs have been bi-oriented and aligned at the metaphase plate, ensuring segregation synchronization and genome integrity [1, 4, 38]. It has been shown that tension regulates phosphorylation of kinetochore substrates [39], such as Dam1 and Ndc80 [13] (figure 2), and hence attachment stability, by modulating the distance between Ilp1/Aurora B kinase and kinetochores [40]. On the molecular level tension and cohesion are mediated and regulated by factors, such as cohesin, Sgo1, Rad61/Wapl, Eco1 and Mec1 [4, 14–16, 34, 41–43]. However, in addition to their functions these molecules and all other factors must comply with equations (2) and (5) and can hence be regarded as enslaved by the collective spindle–SC interaction (equation (9)).

6. A mapping from attachment to collective interaction

In this model the order parameter φ approaches $2N$ continuously, because the density of stably attached kinetochores ψ_s is a continuous variable, implying that segregation erroneously seems to occur promptly once all SC pairs have been bi-oriented and aligned. However, in reality φ and hence also tension and cohesion change with the increasing number of stably attached kinetochores in a discrete stepwise manner. The collective spindle–SC interaction thus predicts a stepwise partial removal of cohesion already during metaphase, without proteolytic cleavage of cohesin molecules which can then be relocated to the chromatin [34]. Anaphase starts with bi-orientation of the last SC pair ($\varphi = 2N$) followed by the observable oscillatory relaxation of the last portion of tension. This suggests that concomitant conformational changes in the MCC complexes might reposition Cdc20 such that APC becomes activated [44], the protecting protein securin destroyed and cohesin cloven by the protease separase [45].

The dependence of φ on ψ_s is obtained by eliminating the explicit dependence on time of the shifted order parameter solution $\varphi(t) = N(1 + \tanh(kagt))$ and of equation (3). But whereas equations (1)–(3) admit the start of stable attachment at $t = 0$, in $\varphi(t)$ this can start already at some large negative time $t \approx -t_0$, $t_0 \gg 1/kag$. Accordingly, the difference, which is just the constant term $\varphi(0) = N$, can be accounted for by shifting time in $\varphi(t)$, $t \to t - t_0$. By insertion of equation (3), $\varphi(t)$ can then be written as a dose–response function, $\varphi(\psi_s) = 2N(\rho'/\sigma')/((\rho'/\sigma') + E(t_0))$, where $E(t_0) = (\rho_K/\sigma_K)\exp(2kagt_0) = (\rho_K/\sigma_K)\exp(k(\rho_K - \sigma_K)t_0)$ accounts for the time lag. The dynamic reactant densities $\rho'(t) = \rho_{R0} - \psi_s(t)$ and $\sigma'(t) = \sigma_{R0} - \psi_s(t)$ are here defined as before, however, with 'renormalized' initial densities, $\rho_{R0} = \rho_K - \psi_u$ and $\sigma_{R0} = \sigma_K - \psi_u$. Unstable attachments are then given a role as background to which SC pairs are exposed (figures 3), like a medium that braces the stably connected part of the spindle–SC system. In the limit $k' = 0$, where also $\psi_u = 0$, the renormalized densities too attain the bare values, $\rho_{R0} \to \rho_K \to \rho_0$ and $\sigma_{R0} \to \sigma_K \to \sigma_0$.

The order parameter, which can also be written as $\varphi(\psi_s) = 2N(\rho_{R0} - \psi_s(t))/(\sigma_{R0} - \psi_s(t))/((\rho_{R0} - \psi_s(t))/(\sigma_{R0} - \psi_s(t)) + E(t_0))$, provides a coarse-grained mapping from the molecular level, at which MT plus-ends attach vacant kinetochores and the density $\psi_s(t)$ is the so-called reaction coordinate, to the collective level at which the number of stable attachments φ is counted and the all-or-none decision to segregate the SC pairs is made. This takes place at $\psi_s = \sigma_{R0}$ ($\sigma' = 0$) when all kinetochores are stably attached by MTs, $\varphi(\sigma_{R0}) = 2N$, as required by the spindle checkpoint premises. As $\rho_K \gg \sigma_K$ it follows that $E(t_0)$ is large and $\varphi(0) \approx 0$ as required by a realistic spindle–SC interaction, $\varphi(\psi_s)$ here denoting just the number of stably attached kinetochores. The contribution $\Delta\varphi \sim \varphi_u$ of unstable attachments, which cause polar ejection forces, was removed from φ by the shift $\xi \to -1 + \xi$, ($\varphi \to -N + \varphi$), hence $\Delta\varphi = N$.

The order parameter $\varphi(\psi_s)$ thus enables the spindle–SC system to sense and count the number of stably attached kinetochores, to sense the critical threshold for segregation at $\varphi = 2N$, and hence to distinguish budding yeast ($N = 16$) from human cells ($N = 46$) and others. Equation (8) shows that polar ejection forces dominate the collective interaction before $\varphi = N$, ($\xi = 1$), where $F = 0$, after which tension takes over and makes the average force $F(\xi)$ repulsive.

7. Comparison with single DNA molecule formula

An interesting question is if the force $F(\xi)$ generated in centromeric chromatin can be related to the force-extension formula obtained by stretching a single DNA molecule in the laboratory [21]. Obviously, stretching DNA by an external force is not what happens in living cells and chromatin in SC pairs contains more than just DNA, e.g. cohesin and histone. However, the decrease in tension and concomitant removal of cohesin (i.e. of tension and cohesion) is controlled by $\varphi(\psi_s)$ and the histone content is accounted for by the elastic modulus [37]. From these aspects a comparison should be possible. If tension in the spindle–SC system were created by an external force the spatial coherence should be violated and the system be less correlated. As the spatial coherence in the actual system is very fragile, the major contribution to the incoherent correction to $F(\xi)$ in equation (9) should contain no correlations. Accordingly, as spatial correlations are associated with nonlinear forces, the incoherent correction term should be linear in ξ, $\Delta F(\xi) = -\kappa'\xi$ and the difference between κ' and $\kappa = 4D^2\varepsilon g^2/\Delta^2$ should be due to modifications of D and Δ by the external force.

One complicated way to obtain κ' would be to derive the model from equation (4) with $\Delta r_\lambda \neq 0$ and then subtract the coherent part defined by equation (9). A simpler feasible way is to estimate how Δ and D are modified by the external force. Thus, Δ in $\kappa = 4D^2\varepsilon g^2/\Delta^2$ should be replaced by a spacing proportional to the average stretch χ hence $\Delta^2 \to \langle\chi_\lambda\rangle^2 = \chi^2 = D^2\xi^2$. However, the force $F(\xi)$ was obtained by the displacement $\xi \to -1 + \xi$. To be compatible with $F(\xi)$ in equation (9), Δ^2 should therefore be replaced by $D^2(1 - \xi)^2$

which corresponds to a shift $\langle(-D+\chi_\lambda)\rangle^2$ in the discrete lattice.

Secondly, D^2 should be replaced by $\langle \boldsymbol{R}_\lambda^2\rangle = \Sigma(\boldsymbol{R}_\lambda^2)/2N = R_g^2$, R_g being the radius of gyration [46] and $\boldsymbol{R}_\lambda = (\pm R_\lambda, 0, 0)$ the vector from centre of mass $\boldsymbol{r}_{cm} = (0,0,0)$ on the metaphase plate to the stably attached kinetochores where plus and minus apply to right- and left-oriented chromosomes, respectively. As $R_g^2 = L_m^2/6$ [46, 47], where L_m^2 is the mean square end-to-end length of the cluster-shaped lattice, and L_m should equal the average stretch χ, D^2 should be replaced by $D^2\xi^2/6$. However, to be compatible with $F(\xi)$ in equation (9), $\langle \boldsymbol{R}_\lambda^2\rangle$ should be correspondingly shifted by $\boldsymbol{D} = (D,0,0)$ in the discrete lattice. Hence, as $\langle \boldsymbol{D}\cdot\boldsymbol{R}_\lambda\rangle = \boldsymbol{D}\cdot\boldsymbol{r}_{cm} = 0$, it follows that $D^2 \to \langle(-\boldsymbol{D}+\boldsymbol{R}_\lambda)^2\rangle = D^2 + R_g^2 = D^2(1+\xi^2/6)$, the first term being the harmonic force in equation (9). Thus, with both Δ and D corrected the force becomes

$$F_c(\xi) = \frac{\kappa C}{2(1-\xi)^2}(\xi(1-\xi)(2-\xi)+\xi^3/3) \propto \frac{k_B T}{p}\left(\xi + \frac{1}{4(1-\xi)^2} - \frac{1}{4}\right), \tag{10}$$

where $C \sim \Delta^2/D^2$ hence $\kappa C \sim 4\varepsilon g^2 \sim 3k_B T/b_K$, k_B is Boltzmann's constant, T temperature, $b_K = 2p$ the effective Kuhn segment length and p the persistence length. Equation (9) thus provides a relationship between the force-extension formula assessed on a single DNA molecule [21], i.e. the worm-like chain (WLC) model [48], and the collective spindle–SC interaction (equation (9)). It is also noteworthy that the collective interaction is formally identical to the earlier obtained DNA–protein dynamics for replication initiation [49] provided that the attachment of licencing proteins to origins of DNA replication is described as a travelling wave with velocity Δka.

8. Summary and outlook

A non-equilibrium collective spindle–SC interaction, which seems to explain the most essential properties and functions of the spindle checkpoint machinery, has been obtained. The model is founded on the non-equilibrium attachment reaction of MT plus-ends to vacant kinetochores (equation (1)), which describes how the density of stably attached kinetochores increases, and on the spatial correlations between such kinetochores (equation (5)), which makes the spindle–SC system increasingly rigid. These two conditions in combination with the initial boundary constraints for the two key reactant densities uniquely determine the form of the spindle–SC interaction. The spatial correlations make the average force (equation (9)) on and between kinetochores (figure 2) nonlinearly dependent on the increasing number of stably attached kinetochores. In the absence of stable attachments ($\xi = 0$) and after completed bi-orientation ($\xi = 2$) the collective average force $F(\xi)$ is exactly equal to the factual, although vanishing, tension. However, already at $\xi = 2 - 2/N$ when $N-1$ SC pairs are bi-oriented $F(\xi)$ equals approximately the factual tension and hence also the factual cohesion which balances the tension (figure 2), because then only one SC pair remains to come under tension. Near the anaphase entry the collective force thus describes how tension and cohesion decrease nonlinearly with the increasing number of stably attached kinetochores [4] and thus how the remaining amount of tension becomes equally shared between bi-oriented SC pairs. This implies a corresponding equal sharing of the remaining amount of cohesion, ensuring stability of all bi-oriented SC pairs [6, 13] and blocking of segregation in metaphase. It also ensures a simultaneous vanishing of tension and cohesion, and hence a synchronized segregation and genome integrity [1, 4, 38]. The model thus seems to confirm the current belief that the spindle checkpoint monitors the spindle–SC interaction [4]. However, with continuously changing ψ_s and $\varphi(\psi_s)$, a consequence of continuously variable volume average reactant densities which are insensitive to detailed regulations on timescales shorter than the spindle assembly, the spindle–SC interaction is unable to differ between the non-relaxed state at completed bi-orientation, and the relaxed state with separated SCs and zero tension. But in reality $\varphi(\psi_s)$ changes in a discrete stepwise manner, which leads to an oscillatory relaxation in anaphase as will be further discussed here.

When $\varphi(\psi_s)$ increases, tension decreases and the collective spindle–SC interaction enforces an equal decrease in cohesion, i.e. a corresponding removal of cohesin molecules in the SC pairs. Conversely, in cases when $\varphi(\psi_s)$ decreases $F(\xi)$ enforces a genome-wide increase in tension and hence in cohesion, implying that the model predicts a corresponding recruitment of cohesin to SC pairs in a genome-wide manner. In fact, this effect has been observed already in the case of a single double-strand break (DSB) in DNA. Surprisingly, large amounts of cohesin were then recruited not only to the SC pair with damaged DNA but also to the undamaged SC pairs, strengthening the cohesion in the entire genome [38, 42, 43]. The collective spindle–SC interaction thus provides an explanation also of this miraculous effect. Cohesin recruited to the damaged chromosome increases the difference between the damaged SC pair and the others, thereby reducing the number of identical (undamaged) stably attached kinetochore–SC complexes by two units. According to equation (9), $F(\xi)$ and hence tension and cohesion then increase in a genome-wide manner, which on the molecular level is accomplished by a compensatory recruitment of cohesin also to undamaged SC pairs, blocking segregation until the DSB repair is finished. From a physical point of view this is not a miracle.

What happens is that the spindle checkpoint machinery works on two levels. On the molecular level forces acting on individual SC pairs are generated by molecular motors and depolymerizing MTs [27, 28]. However, apart from actions on the molecular level, these two factors and regulators and mediators of tension and cohesion, such as Ilp1/Aurora B, cohesin, Sgo1, Rad61/Wapl, Eco1 and Mec1 [4, 14–16, 34, 40–43], as well as dynamic and directional instabilities [10, 25, 29–31], kinetochore oscillations and all other molecular factors, must comply with the enveloping conditions, equations (1) and (5) and the boundary constraints. Consequently, all molecular functions are obliged to comply with equation (9), implying that the entire system, separate

compartments and components and their functions are enslaved by the collective spindle–SC interaction regardless of if φ decreases or increases.

This type of Ginsburg–Landau model has been employed before to study slow dynamic behaviour of chemical non-equilibrium systems, however, only in the absence of spatial correlations [50, 51]. In contrast to inanimate condensed matter, in which phase transitions are typically controlled by temperature-dependent order parameters (thermotropic systems) [19], the metaphase-to-anaphase transition is regulated by the number of stable attachments, i.e. by the order parameter $\varphi(\psi_s)$ which depends non-linearly on the density of stably attached kinetochores ψ_s (lyotropic system) [19]. Beside the spatial correlations (equation (5)) and the initial boundary constraints, the normalization of $\varphi(\psi_s)$ by topological quantization [32] is another prerequisite for the spindle–SC system to sense and count the number of stably attached kinetochores and to sense the segregation threshold at $\varphi(\psi_s) = 2N$, and hence for an accurate anaphase entry. The model thus also provides an explanation as to how the cell might be able to count [52, 53] and how the collective spindle–SC interaction can distinguish budding yeast ($N = 16$) from human cells ($N = 46$) and others.

In reality $\varphi(\psi_s)$ and hence tension and cohesion change in a discrete stepwise manner with the increasing number of stable attachments. This induces a genome-wide stepwise decrease in tension and cohesion, ensuring a sufficiently smooth relaxation of tension down to the synchronized removal of the last linkages at the telomeres. Together with a normal telomere function, the stepwise removal of cohesion is thus crucial for a flawless segregation of replicated chromosomes. Bi-orientation of the last SC pair triggers the transition to anaphase in which the remaining amount of tension and cohesion is removed by proteolytic cleavage of the remaining cohesin molecules in the chromosome arms [34, 44, 45]. The corresponding relaxation of tension in centromeric chromatin is mediated by kinetochore oscillations which have been experimentally observed [20]. These oscillations, which take place on a timescale shorter than that required for spindle assembly, were successfully analysed here by a time-dependent perturbation analysis of the collective spindle–SC interaction. That rigidly coupled collections of molecular motors can lead to spontaneous oscillations has been shown also in other model systems [54–57]. However, in the actual case both the oscillatory spectrum and the segregation threshold were derived directly from a self-consistent exactly solvable model, i.e. from the collective spindle–SC interaction, to mention just some differences.

It was thus found that the perturbed collective spindle–SC interaction predicts kinetochore oscillations at a frequency $f \approx (0.88 \pm 0.43)\ \mathrm{min}^{-1}$, which is in satisfactory agreement with the frequency observed about 5 min prior to segregation [20] at $f \approx 1.0\ \mathrm{min}^{-1}$. Segregation is predicted to take place at a threshold 'frequency' $f_{\mathrm{th}} \approx 1.02\ \mathrm{min}^{-1}$ and 'wavelength' $\lambda_{\mathrm{th}} \approx 0.8$ D. The model thus provides explanations as to how the system of stably attached kinetochores/chromosomes could control the spindle checkpoint functions, such as the anaphase onset, and how it might decide to segregate replicated chromosomes [58]. The good agreement between derived and assessed frequencies of kinetochore oscillations and the fact that the oscillatory spectrum also contains a threshold at which SC pairs separate suggest that Cdc20 activation by APC and proteolytic cleavage of cohesin might be mediated by concomitant oscillations in the conformation of the MCC-complex [40, 44, 59, 60]. However, as the collective spindle–SC interaction is just a mean-field theory, the exact numbers obtained for frequencies and wavelengths must be taken with caution.

Apart from providing an extended knowledge about division of normal cells, this model might also improve the understanding of aneuploidy and cancerous cell division. The formal identity of equation (9) with the protein–DNA dynamics governing DNA replication initiation [49], and the loose analogy between the signal transduction network preceding replication initiation and the response induced by DNA damage [61], leads to speculation that one and the same non-equilibrium collective DNA dynamics might be able to control the entire cell cycle by regulating the transitions near and at the checkpoints. Obviously, the key reactants are not the same at all these transitions and the dynamics between the checkpoints is expected to be much more complex. Many questions remain to be further studied, such as the spatial dependence of polar ejection forces and how they contribute to directional instability effects and the transport of SC pairs to the metaphase plate. In the actual model this transport has been treated as a constant time lag without impact on the collective spindle–SC interaction. It also remains to experimentally distinguish directional instability effects (oscillations of SC pairs) from oscillations in the distance between sister kinetochores. The hypothesis that conformational changes in the MCC could mediate the activation of APC by Cdc20 and subsequent proteolytic removal of cohesin, must also be further studied. However, the proposed collective spindle–SC interaction seems to fulfil the most essential spindle checkpoint functions and might hence serve as a platform for continued studies. The relationship defined by equation (10) might help to relate observations in single DNA and chromatin molecule studies to living cell conditions. Moreover, by further studies of living condensed matter systems, the non-equilibrium statistical mechanics defined by equations (1), (2), (5) and the normalization by topological quantization can hopefully be developed to a more general statistical physics theory for 'rigid' non-equilibrium condensed matter systems.

Acknowledgments

I thank Kerry Bloom for information about the experimental results and Mats Jonson, Adrian Parsegian, Danko Radic and Camilla Sjögren for a critical reading of the paper.

References

[1] Pines J 2006 *Trends Cell Biol.* **16** 55
[2] Peters J-M 2007 *Nature* **446** 868

[3] Palframan W J, Meehl J B, Jaspersen S L, Winey M and Murray A W 2006 *Science* **313** 680
[4] Pinsky B A and Biggins S 2005 *Trends Cell Biol.* **15** 486
[5] Mitchison T J and Salmon E D 2001 *Nat. Cell Biol.* **3** E17
[6] Kotwaliwale C and Biggins S 2006 *Cell* **127** 1105
[7] Kline-Smith S L, Sandall S and Desai A 2005 *Curr. Opin. Cell Biol.* **17** 35
[8] Chan G K, Liu S-T and Yen T J 2005 *Trends Cell Biol.* **15** 589
[9] Maiato H, DeLuca J, Salmon E D and Earnshaw W C 2004 *J. Cell Sci.* **117** 5461
[10] Mitchison T and Kirschner M 1984 *Nature* **312** 237
[11] Forer A 1965 *J. Cell Biol.* **25** 95
[12] Bloom K, Sharma S and Dokholyan N V 2006 *Curr. Biol.* **16** R276
[13] DeLuca J G, Gall W E, Ciferri C, Cimini D, Musacchio A and Salmon E D 2006 *Cell* **127** 969
[14] Ben-Shahar T R, Heeger S, Lehane C, East P, Flynn H, Skehel M and Uhlmann F 2008 *Science* **321** 563
[15] Michaelis C, Ciosk R and Nasmyth K 1997 *Cell* **91** 35
[16] Guacci V, Koshland D and Strunnikov A 1997 *Cell* **91** 47
[17] O'Connel C B and Khodjakov A L 2007 *J. Cell Sci.* **120** 1717
[18] Kapoor T M, Lampson M A, Hergert P, Cameron L, Cimini D, Salmon E D, McEwen B F and Khodjakov A 2006 *Science* **311** 388
[19] deGennes P G and Prost J 1993 *The Physics of Liquid Crystals* (Oxford: Oxford University Press)
[20] Pearson C G, Maddox P S, Salmon E D and Bloom K 2001 *J. Cell Biol.* **152** 1255
[21] Bustamante C, Marko J F, Siggia E D and Smith S 1994 *Science* **265** 1599
[22] Lüders J and Stearns T 2007 *Nat. Rev. Mol. Cell Biol.* **8** 161
[23] Doi M and Edwards S F 1986 *The Theory of Polymer Dynamics* (Oxford: Oxford University Press)
[24] Huang K 1987 *Statistical Mechanics* (New York: Wiley)
[25] Levesque A A and Compton D A 2001 *J. Cell Biol.* **154** 1135
[26] Antonio C, Ferby I, Wilhelm H, Jones M, Karsenti E, Nebreda A R and Vernos I 2000 *Cell* **102** 425
[27] Sharp D J, Rogers G C and Scholey J M 2000 *Nat. Cell Biol.* **2** 922
[28] Koshland D E, Mitchison T J and Kirschner M W 1988 *Nature* **331** 499
[29] Rieder C L, Davison E A, Jensen L C W, Cassimeris L and Salmon E D 1986 *J. Cell Biol.* **103** 581
[30] Skibbens R V, Skeen V P and Salmon E D 1993 *J. Cell Biol.* **122** 859
[31] Joglekar A P and Hunt A J 2002 *Biophys. J.* **83** 42
[32] Jackiw R 1977 *Rev. Mod. Phys.* **49** 681
[33] Combs J A and Yip S 1983 *Phys. Rev.* B **28** 6873
[34] Ishiguro K and Watanabe Y 2007 *J. Cell Sci.* **120** 367
[35] Morse P M and Feshbach H 1953 *Methods of Theoretical Physics* (New York: McGraw-Hill)
[36] Portet S, Tuszynski J A, Hogue C W V and Dixon J M 2005 *Eur. Biophys. J.* **34** 912
[37] Bouck C D and Bloom K 2007 *Curr. Biol.* **17** 741
[38] Watrin E and Peters J-M 2007 *Science* **317** 209
[39] Nicklas R B, Ward S C and Gorbsky G J 1995 *J. Cell Biol.* **130** 929
[40] Liu D, Vader G, Vromans M J M, Lampson M A and Lens S M A 2009 *Science* **323** 1350
[41] Indjeian V B, Stern B M and Murray A W 2005 *Science* **307** 130
[42] Ström L, Karlsson C, Lindroos H B, Wedahl S, Katou Y, Shirahige K and Sjögren C 2007 *Science* **317** 242
[43] Ünal E, Heidinger-Pauli J M, Kim W, Guacci V, Onn I, Gygi S P and Koshland D E 2008 *Science* **321** 566
[44] Herzog F, Primorac I, Dube P, Lenart P, Sander B, Mechtler K, Stark H and Peters J-M 2009 *Science* **323** 1477
[45] Uhlmann F, Lottspeich F and Nasmyth K 1999 *Nature* **400** 37
[46] Flory P J 1988 *Statistical Mechanics of Chain Molecules* (New York: Oxford University Press)
[47] Debye P 1946 *J. Chem. Phys.* **14** 636
[48] Marko J F and Siggia E D 1995 *Macromolecules* **28** 8759
[49] Matsson L 2005 *J. Biol. Phys.* **31** 303
[50] Reichl L E 1998 *A Modern Course in Statistical Physics* (New York: Wiley)
[51] Nicolis G and Prigogine I 1977 *Self-Organization in Nonequilibrium Systems* (New York: Wiley)
[52] Smith K A 2005 *J. Biol. Phys.* **31** 261
[53] Smolke C D 2009 *Science* **324** 1156
[54] Derényi I and Vicsek T 1995 *Phys. Rev. Lett.* **75** 374
[55] Jülicher F and Prost J 1995 *Phys. Rev. Lett.* **75** 2618
[56] Derényi I and Ajdari A 1996 *Phys. Rev.* E **54** R5
[57] Jülicher F and Prost J 1997 *Phys. Rev. Lett.* **78** 4510
[58] Inoué S and Salmon E D 1995 *Mol. Biol. Cell* **6** 1619
[59] Stegmeier F, Rape M, Draviam V M, Nalepa G, Sowa M E, Ang X L, McDonald E R III, Li M Z, Hannon G J, Sorger P K, Kirschner M W, Harper J W and Elledge S J 2007 *Nature* **446** 876
[60] Reddy S K, Rape M, Margansky W A and Kirschner M W 2007 *Nature* **446** 921
[61] Petrini J H J 2007 *Science* **316** 1138